Hindawi
Shock and Vibration
Volume 2023, Article ID 6691129, 9 pages
https://doi.org/10.1155/2023/6691129

Research Article

Seismic Vulnerability Analysis of Steel Clarification Tank

Chuyun Cheng,[1] Xiwei Cheng,[2] Wanlin Zhang,[3] Xinhai Zhou,[3] Junliang Hong,[3] and Xuansheng Cheng[3]

[1]*Design School, Xi'an Jiaotong-Liverpool University, Suzhou 215123, China*
[2]*School of Finance and Commerce, Lanzhou Resources & Environment Voc-Tech University, Lanzhou 730021, China*
[3]*Western Engineering Research Center of Disaster Mitigation in Civil Engineering of Ministry of Education, Lanzhou University of Technology, Lanzhou 730050, China*

Correspondence should be addressed to Xuansheng Cheng; chengxuansheng@gmail.com

Received 3 May 2023; Revised 5 July 2023; Accepted 26 August 2023; Published 13 September 2023

Academic Editor: Annalisa Greco

As a physical analysis method, susceptibility not only predicts the probability of failure of a structure under different hazard levels but also prevents disasters induced by structural damage due to vulnerable members. To study the susceptibility of steel clarification tank under earthquake action, this study analyzes the dynamic response of steel clarification tank under near-field impulse, near-field no impulse, and far-field ground shaking, derives IDA curve clusters by incremental dynamic analysis method, and conducts related studies to analyze the susceptibility of clarification tank structures through susceptibility curves. The results of the study show that the probability of failure of the clarification tank under different ground shaking intensities is different. The probability of liquid wave height transcendence of the clarification tank under seismic action is the largest, the probability of liquid wave height transcendence of the clarification tank under near-field pulsed seismic action is the second, the probability of liquid wave height transcendence of the clarification tank under near-field nonpulsed seismic action is the smallest, and the probability of transcendence occurs similarly in near-field pulsed and far-field seismic actions.

1. Introduction

The probability of a certain degree of damage to a steel clarification tank under different ground shaking responses, i.e., fragility, is a probabilistic event. Fragility can not only predict the components and location of structural damage of steel clarification tank but also prevent disasters induced by structural damage due to fragile components. Therefore, many scholars have studied fragility to determine the location of structural damage under earthquake conditions, which has become a method to determine the damage of structures under earthquakes in many studies, is widely used to identify the reliability of steel clarification tank under earthquakes, and is also used to determine the seismic resistance of steel clarification tank.

Kong et al. [1] obtained the susceptibility curves under each performance parameter through a large number of nonlinear finite element simulations and analyzed the probability of dam damage under seismic effects of different intensities. Based on the energy density and maximum plastic strain criterion, Zhao et al. [2] established the limit state equations for the damage failure of chemical storage tanks under the coupled action of explosion shock wave and debris. Chen et al. [3, 4] established the limit state equation for the target liquid storage tank under the coupled action of temperature load and explosive fragment impact load and analyzed the influence law of explosive fragment mass, impact velocity, and impact angle on the vulnerability of the target liquid storage tank under different tank wall temperatures. Ye et al. [5] calculated the various susceptibility parameters of the tank to derive the damage curve to analyze the low failure probability values. Aliche et al. [6] used the concept of natural hazard vulnerability based on the vulnerability index (I-V) assessment to predict the possible degradation and aging of the tank structure. Wei et al. [7] analyzed the form of the relationship between seismic acceleration and the degree of damage to the storage tank by using probabilistic estimation. Qi [8] plotted the

vulnerability curves of vaulted tanks under explosive fragments by the finite element method for large vertical liquid storage tanks sampled and calculated. Sun et al. [9] introduced a probability model of random variables and a failure probability calculation method based on susceptibility theory and concluded that multiple failure modes for seismic susceptibility study of liquid storage tanks are more scientific than susceptibility study from a single failure mode. Li [10] studied the seismic damage characteristics of liquid storage tanks and determined the failure mode and damage criterion of liquid storage tanks accordingly. Rong et al. [11] performed an incremental dynamic analysis of the containment structure by establishing a refined finite element model. Vamvatsikos and Cornell [12] analyzed the seismic capacity of the structure statistically by amplitude modulation of selected multiple seismic waves and by many dynamic responses using incremental dynamic analysis to make the structure go through from elastic to inelastic phase. Lu et al. [13] did dynamic elastoplastic time analysis to calculate and analyze the whole process of the structure under the action of different ground shaking intensities in going through elastic and elastoplastic phases and finally to collapse thus deriving the vulnerability results. Zhang [14] used the damage state of a liquid storage tank to calculate the failure mode of the structure and to study the susceptibility and failure probability of the structure. The methods that can be used to perform structural susceptibility analysis include the expert discrimination method, empirical analysis method, analytical method, and hybrid method, among which Razzaghi and Eshghi [15] evaluated the susceptibility of steel storage tanks by using analytical and empirical analysis methods to analyze the safety of the structure and studied that the height-to-diameter ratio and liquid storage volume are the main indicators affecting the susceptibility of the storage tanks. Phan et al. [16] analyzed the seismic susceptibility of a high-level steel storage tank supported by reinforced concrete frame columns and finally concluded that PGA is the most effective seismic strength indicator. Zhang et al. [17] studied the dynamic properties of the structure by numerical simulation and further analyzed the damage mechanism of the structure, concluding that the tank wall was compressed along the annulus and tensioned along the axial direction during the dynamic response.

In summary, seismic performance analysis can effectively estimate the hazard of a structure under earthquake action, and many scholars have studied the susceptibility to damage to determine the location of structural damage under earthquake conditions. In order to study the susceptibility of steel clarification tank under seismic waves, this study analyzes the seismic capacity of steel clarification tank by using near-field impulse seismic waves, near-field no-impulse seismic waves, and far-field seismic waves for dynamic response analysis, analyzes the seismic capacity of steel clarification tank by IDA curve clusters, and studies the susceptibility of steel clarification tank based on the susceptibility method, which has guiding significance for the structure in terms of higher stress and member destabilization damage.

2. Analytical Model and Parameter Setting

In this paper, the finite element method is used to analyze the clarification tank. The schematic diagram is shown Figure 1. The parameters are selected in Table 1. The body of the clarification tank is a steel structure. The diameter of the outer tank is 11.50m, the diameter of the inner tank is 3.65m, and the height is 10.50m. The main components include the guide plate, reaction barrel, water collection tank, fender, and other components for the steel plate. The finite element software ADINA is used. The wall, inner barrel, cone, and bottom of the clarification tank are divided into shell elements. In order to make the numerical simulation results more accurate, the cell mesh size is less than 1/10~1/8 wave length, and the three-dimensional finite element analysis model is obtained, as shown in Figure 2.

3. Failure Criterion of Steel Clarification Tank

Steel clarification tank as a special structure, the peak of liquid shaking will be too large to cause the outflow of liquid, which will lead to disaster, considering the special characteristics of the clarification tank, using the following failure criterion [18].

3.1. Liquid Shake Height Limit (H_{limit}). The liquid in the clarification tank will sway under the excitation of the seismic wave. If the reserved dry chord height does not exceed the maximum height of the liquid sloshing peak, the liquid will overflow from the clarification tank, causing secondary disasters and certain economic losses. Therefore, it is very important to set the liquid sloshing peak as the failure criterion. The failure criterion is as follows:

$$H < H_{\text{limit}}, \tag{1}$$

where H is the liquid sloshing height and H_{limit} is the distance from the static liquid level to the top of the panel, which is the dry chord height.

3.2. Structural Displacement Limit (S_{limit}). The structure of clarification tank will produce a large horizontal displacement S under the action of an earthquake. When a rare earthquake is encountered, the structural displacement S will be larger. Selecting the displacement limit S_{limit} of the clarification tank as the failure criterion not only has a guiding effect on the damage of the structure but also has important judgment significance for the outflow rate of liquid under the cracking of the structure.

$$S < S_{\text{limit}}, \tag{2}$$

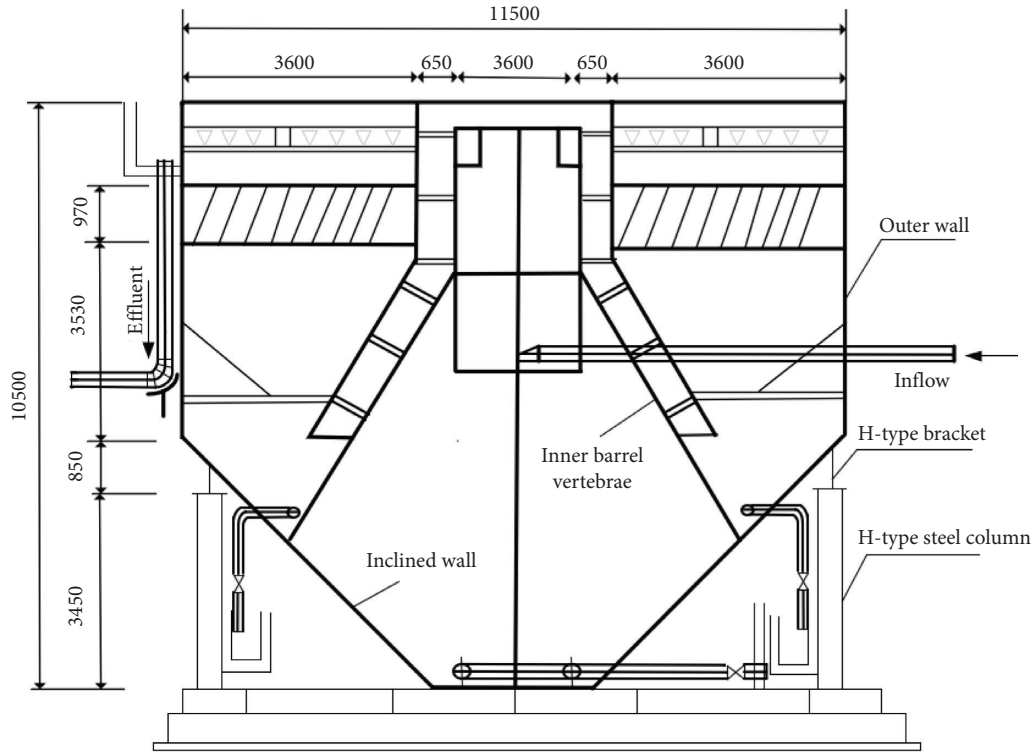

Figure 1: Schematic diagram of clarification tank structure.

Table 1: Model parameters.

Parameters	Numerical value
Elastic modulus	$E = 2.1 \times 10^{11}$ Pa
Poisson ratio	$\mu = 0.3$
Density	$\rho = 7800\ \text{kg/m}^3$
Acceleration of gravity	$g = 9.8\ \text{m/s}^2$

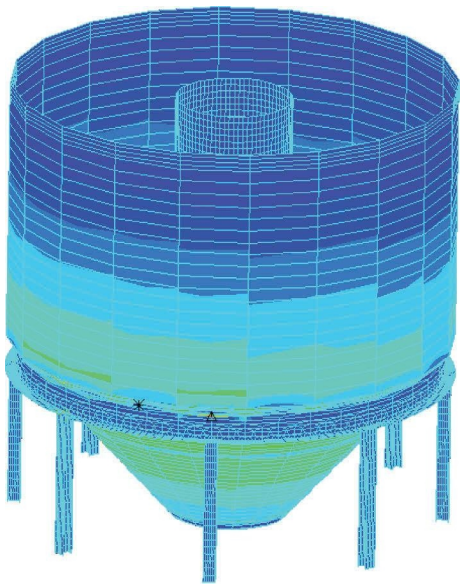

Figure 2: 3D finite element analysis model diagram.

where S is the structural displacement and S_{limit} is the maximum structural displacement [18].

3.3. Vulnerability Analysis Method. Vulnerability refers to the probability that the structure reaches or exceeds a certain limit state under different intensity earthquakes, or the possibility of some degree of damage to the structure due to the occurrence of earthquakes. At present, the methods that can be used for structural vulnerability analysis mainly include expert discrimination method, empirical analysis method, analytical method, and mixed method. The main steps of structural vulnerability analysis based on the analytical method are as follows:

(a) Select a certain number of seismic records, gradually increase the seismic intensity, and perform incremental dynamic analysis on the structure in turn.

(b) Determine the index PI that can reflect the structural failure (failure) state, and define a reasonable value PI_i.

(c) The probability P of structural damage DM exceeding the damage index PI_i under earthquakes with different intensities IM_i is calculated. The existing research shows that the probability distribution of structural damage DM conforms to the lognormal distribution. The advantage of this assumption is that it can provide mathematical convenience for the uncertainty and randomness of

structural seismic capacity and seismic demand. The details can be expressed as follows:

$$P\left(DM \geq PI_i \middle| IM = IM_i\right) = 1 - P\left(DM \leq PI_i \middle| IM = IM_i\right) = 1 - \Phi\left[\frac{\ln PI_i - \mu_{\ln DM|IM=IM_i}}{\sigma_{\ln DM|IM=IM_i}}\right], \tag{3}$$

where $\mu_{\ln DM|IM=IM_i}$ and $\mu_{\ln \mathrm{DM}|\mathrm{IM}=\mathrm{IM}_i}$ are the log mean and log standard deviation of the structural damage DM when $IM = IM_i$. $\Phi(\bullet)$ is the standard normal cumulative distribution function.

(d) Taking the ground motion intensity index IM as the abscissa and the exceedance probability P as the ordinate, the seismic vulnerability curve of the structure can be obtained by fitting the data points with statistical methods.

3.4. Critical Amplitude. Regarding the sloshing wave height of the fluid in the liquid storage structure, the "Standard for seismic design of petrochemical steel equipments" (GB50761-2012) [19] stipulates

$$\begin{aligned} H &= 1.5kaR, \\ k &= 0.18T^2 - 0.326T + 1.697, \end{aligned} \tag{4}$$

where k is the long-period response spectrum coefficient, T is the basic period of fluid sloshing, and a is the seismic influence coefficient.

4. Ground Motion Information

In order to study the incremental dynamic analysis and vulnerability of steel clarification tank, a certain number of seismic waves are selected under different types of near-field pulse, near-field nonpulse, and far-field seismic waves. In order to reduce the influence of seismic wave uncertainty on IDA (increment dynamic analysis) analysis of clarification tank, 10 seismic waves are randomly selected under different types of seismic waves for analysis and research to obtain relatively accurate and reliable evaluation and judgment results.

5. Vulnerability Analysis

5.1. IDA Curve Cluster of Clearing Tank under Near-Field Pulseless Seismic Wave. In order to analyze the clarification tank structure and liquid under near-field no-pulse, 10 seismic waves are selected from the near-field database, as shown in Table 2. In order to analyze the vulnerability and incremental dynamic analysis more accurately, PGA (peak acceleration of earthquake) is used to indicate the intensity index, and then, the amplitude of the seismic waves is adjusted, so that the PGAs are gradually adjusted from 0.1 g to 1.0 g, and each adjustment increases by 0.1 g for a total of 10 times, and then, the finite element software is applied in near-field no-pulse seismic action on the clarification tank in the full water state, the maximum stress, maximum displacement, and the maximum peak of liquid shaking are recorded, and then, the data are organized, respectively, and IDA curve clusters of structural stress, IDA curve clusters of structural displacement, IDA curve clusters of wave height, and IDA curve clusters under near-field no-pulse seismic waves are shown in Figure 3.

It can be seen from Figure 3 that the IDA curve shows a differentiation trend after the maximum structural stress of the clarification tank is PGA 0.4 g; after the liquid sloshing wave height is PGA >0.1 g, the IDA curve differentiation phenomenon appears, and the differentiation is more uniform, reflecting that the selection of near-field nonpulse seismic waves is random, and the evaluation results will be more accurate.

5.2. IDA Curve Cluster of Clearing Pond Structure under Near-Field Impulse Earthquake. In order to analyze the structure and liquid of the clarification tank under near-field pulsed, 10 seismic waves are selected from the near-field pulsed database, as shown in Table 3, and the intensity index is expressed by PGA, and then, the amplitude of the seismic waves is adjusted, so that the PGAs are gradually adjusted from 0.1 g to 1.0 g, and each adjustment increases by 0.1 g, for a total of 10 times, and the finite element software is applied to the clarification tank filled with water under near-field pulsed seismic action. By the calculation, the IDA curve clusters of structural forces, structural displacements and wave height under near-field pulse seismic wave are shown in Figure 4.

As can be seen from Figure 4, the structural maximum stress of the clarification tank is basically similar to the structural interlayer displacement response at PGA <0.1 g; the structural displacement of the clarification tank shows IDA curve divergence after PGA >0.2 g; the shaking wave height of the liquid shows IDA curve divergence after PGA >0.1 g, and the divergence is basically uniform except for the rest at the beginning, reflecting the selection of near-field with pulsed seismic waves with randomness, and the assessment results will be more accurate.

5.3. IDA Curve Cluster of Clearing Pond Structure under Far-Field Earthquake. In order to analyze the structure and liquid under the action of the far-field earthquake, 10 seismic waves are selected from the far-field database, as shown in Table 4. In order to analyze the susceptibility and incremental dynamic analysis more accurately, PGA is used to indicate the intensity index, and equal steps of amplitude

Table 2: Near-field pulseless seismic wave.

Numbers	Name of seismic wave
1	El Centro
2	Victoria-Victoria Hospital Sotano
3	Victoria-Chihuahua
4	Corinth-Corinth
5	Parkfield-Cholame-Shandon Array #8
6	Morgan Hill-Gilroy Array #4
7	Parkfield-Cholame-Shandon Array #12
8	Loma Prieta-Capitola
9	Loma Prieta-Gilroy Array #4
10	Imperial Valley-06-Calexico Fire Station

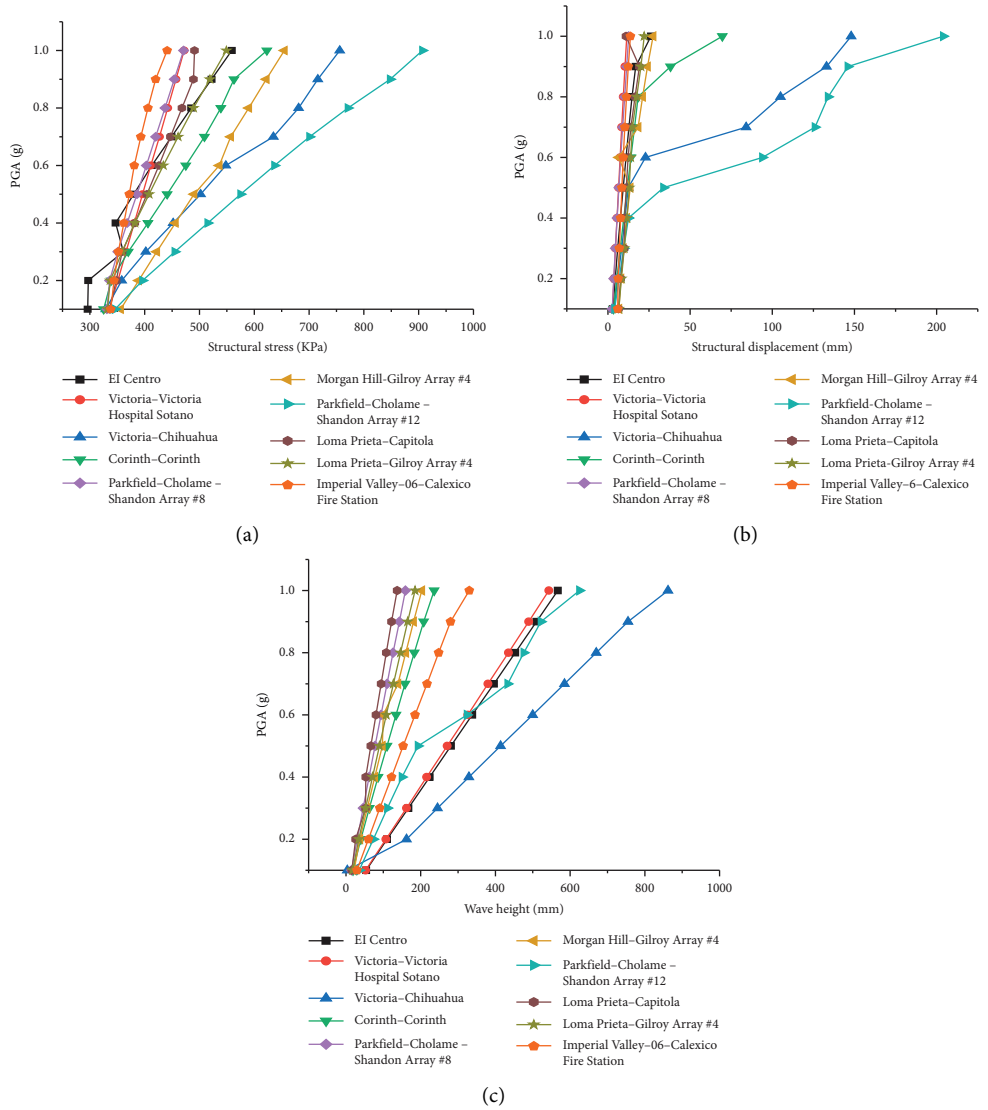

Figure 3: IDA curve cluster of the maximum dynamic response of clarification tank in near-field without pulse. (a) Structural stress. (b) Structural displacement. (c) Wave height.

modulation are performed for each ground shaking, so that the change range of its PGA is 0.1 g~1.0 g, and the increase was 0.1 g for the far-field earthquake action on the clarification tank. The maximum force, maximum displacement, and maximum peak of liquid shaking are calculated under the state of full water and recorded, and then, the data are collated, and the IDA curve clusters of structural force, IDA curve clusters of structural

Table 3: Near-field pulse seismic wave.

Numbers	Name of seismic wave
1	Cape Mendocino-Centerville BeacHNaval Fac
2	Imperial Valley-06-Brawley Airport
3	Imperial Valley-06-EC County Center FF
4	Irpinia-Sturno (STN)
5	Loma Prieta-Gilroy-Historic Bldg
6	Loma Prieta-Gilroy Array #2
7	Loma Prieta-Gilroy Array #3
8	Loma Prieta-Saratoga-Aloha Ave
9	Northridge-01-Pardee-SCE
10	Superstition Hills-02-Kornbloom Road (temp)

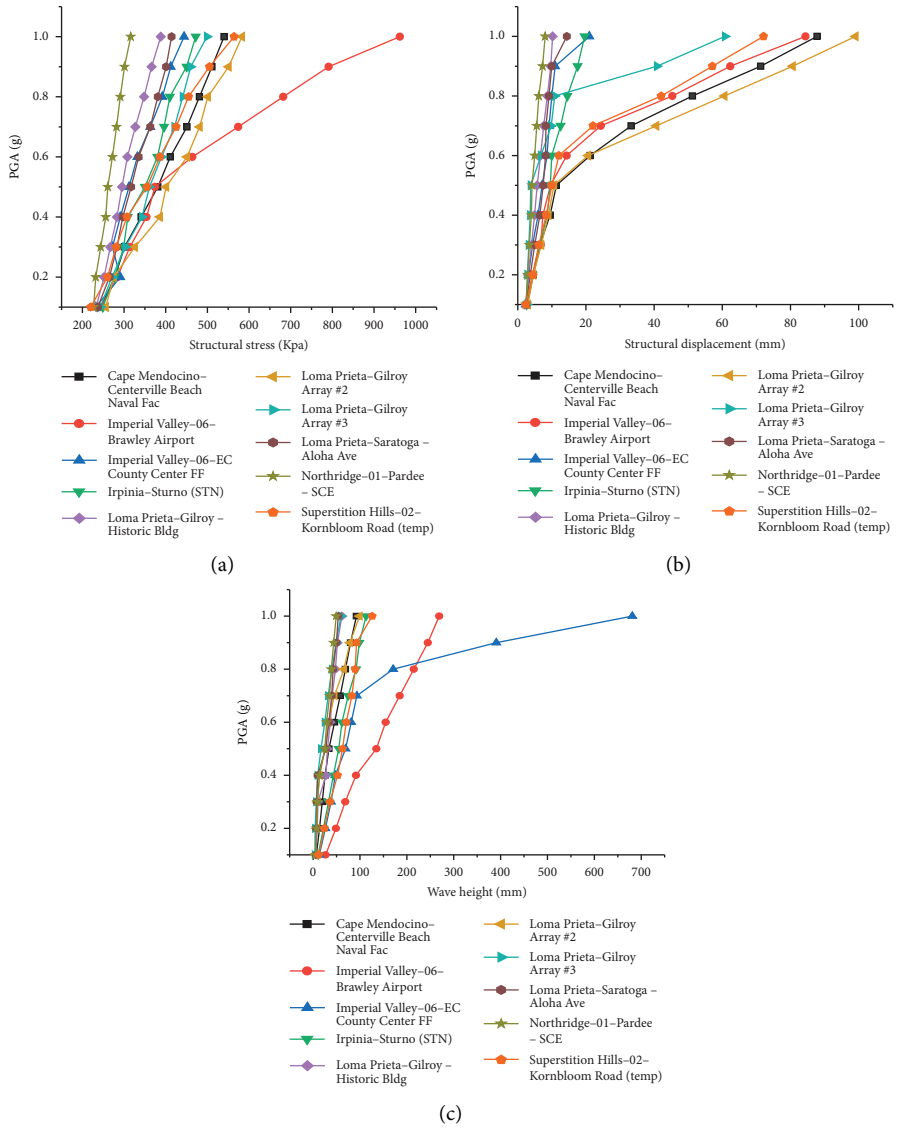

Figure 4: IDA curve cluster of maximum dynamic response of clarification tank under near-field pulse. (a) Structural stress. (b) Structural displacement. (c) Wave height.

displacement, and IDA curve clusters of wave height are plotted, respectively, and the IDA curve clusters under the action of far-field earthquake are shown in Figure 5.

From Figure 5, it can be seen that the maximum stress of the structure of the clarification tank is after PGA 0.2 g, and the IDA curve differentiation phenomenon appears after the

Table 4: Far-field seismic wave.

Numbers	Name of seismic wave
1	Borrego-El Centro Array #9
2	Chi-Chi-CHY044
3	Dinar-Balikesir
4	Friuli_Italy-01-Conegliano
5	Ierissos_Greece-Ierissos
6	Imperial Valley-06-Plaster city
7	Irpinia_Italy-01-Arienzo
8	Kobe-TOT
9	Parkfield-San Luis Obispo
10	San Fernando-Fort Tejon

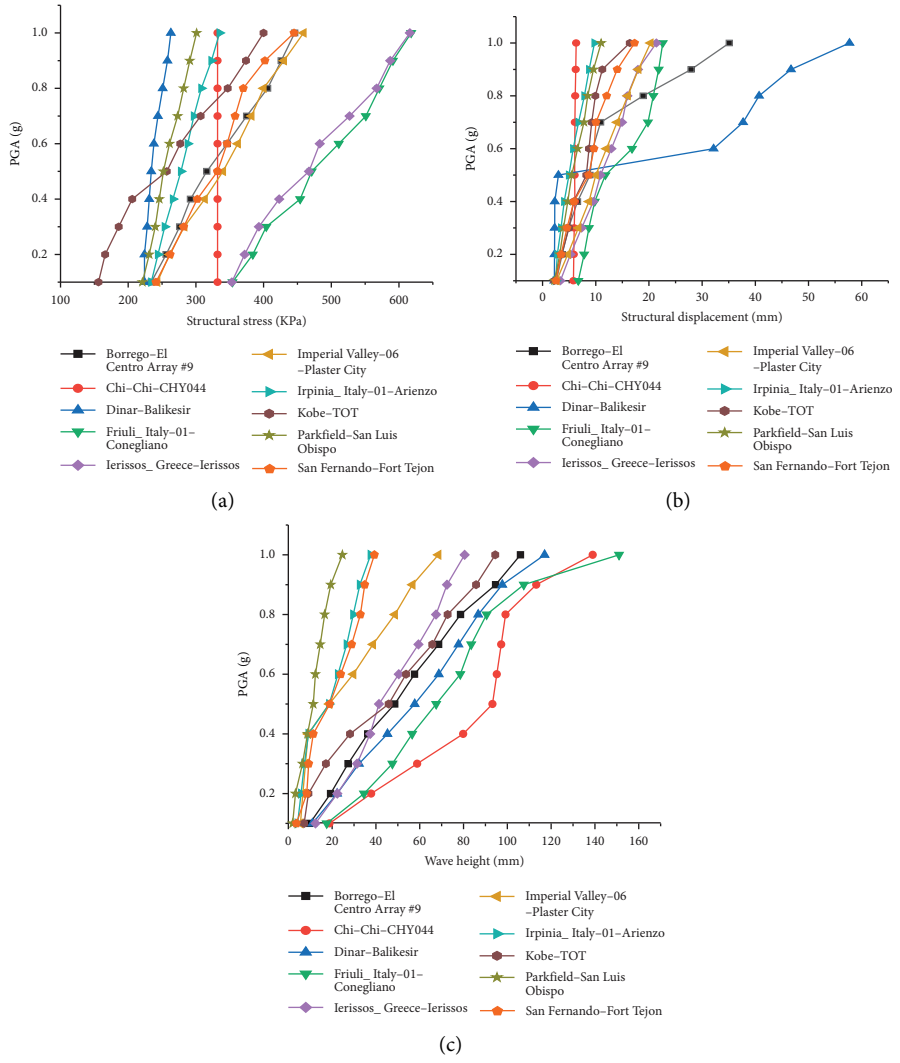

Figure 5: IDA curve cluster of maximum dynamic response of clarification tank in far field. (a) Structural stress. (b) Structural displacement. (c) Wave height.

sloshing wave height of the liquid is PGA >0.1 g, and the IDA curve differentiation phenomenon occurs, and the rest is basically uniform except for a few at the beginning of differentiation, indicating that the selected far-field ground motion considers the randomness of ground motion, and the vulnerability curve is shown in Figure 6.

As can be seen in Figure 5, the PGA for the clarification tank with 100% probability of exceedance under near-field pulsed and far-field seismic waves is roughly 0.50 g. Under near-field unpulsed seismic waves, the PGA with 60% probability of exceedance is roughly 0.20 g. The exceedance probability of steel clarification under far-field seismic wave

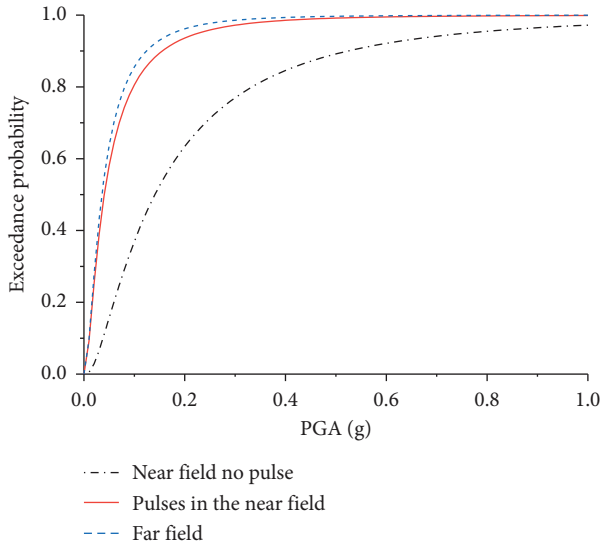

Figure 6: Fragility curve.

response is the largest category under the three different types of waves, and the exceedance probability of steel clarification under near-field unpulsed seismic action is the smallest. In the near-field pulsed and far-field seismic waves, the transcendence probability of steel clarification under these two types of seismic waves is very close; among the three types of seismic waves selected, the transcendence probability of damage occurs when the PGA reaches and exceeds 1.0 g. From this aspect, it is inferred that the probability of damage to the clarification tank under particularly large seismic waves is very high, and in order to prevent the clarification tank from breaking the ring due to the earthquake, it is very important to prevent the damage of the clarification tank by some strengthening measures. It is very necessary to prevent the damage to the clarification tank by some strengthening measures. Compared with the research results [18], the results are consistent with the research results, which prove the reliability of the research results.

6. Conclusions

(1) Under the near-field pulse ground motion response, the stress of the clarification tank structure is basically similar when PGA <0.1 g. After PGA >0.4 g, the IDA curve of the structural displacement of the clarification tank showed a differentiation trend. After the sloshing wave height of the liquid in the clarification tank is PGA >0.1 g, the IDA curve differentiation occurs, and the differentiation is more uniform.

(2) Under the near-field ground motion without a pulse, the interstory displacement response of the structure is similar when PGA <0.1 g. After PGA >0.2 g, the IDA curve differentiation phenomenon appeared in the structural displacement of clarification tank. After PGA >0.1 g, the IDA curve differentiation phenomenon appears in the sloshing wave height of the clear tank liquid.

(3) Under the far-field seismic response, the structural displacement response of the clarification tank is basically similar when PGA <0.1 g; after PGA >0.2 g, the IDA curve differentiation phenomenon appeared in the structural displacement of clarification tank. When PGA >0.1 g, the IDA curve differentiation phenomenon appears in the liquid sloshing wave height of the clarifying tank.

(4) The failure probability of the clarification tank is different under different ground motion intensities, and the exceeding probability of the liquid wave height of the clarification tank under the far-field earthquake is the largest, the exceeding probability of the liquid wave height of the clarification tank under the near-field pulse earthquake is the second, and the exceeding probability of the liquid wave height of the clarification tank under the near-field nonpulse earthquake is the smallest. The exceeding probability of near-field pulse and far-field earthquake is similar.

Data Availability

All data, models, and code generated or used during the study are available in the submitted article.

Conflicts of Interest

The authors declare that they have no conflicts of interest.

Acknowledgments

This research was supported in part by the National Natural Science Foundation of China (grant number 51968045).

References

[1] X. J. Kong, R. Pang, D. G. Zou, B. Xu, and Y. Zhou, "Seismic performance evaluation of high CFRDs based on incremental dynamic analysis," *Chinese Journal of Geotechnical Engineering*, vol. 40, no. 6, pp. 978–984, 2018.

[2] J. Zhao, E. Lai, and G. H. Chen, "Study of vulnerability of chemical storage tank subjected to coupling effect of blast wave and fragment," *Journal of South China University of Technology*, vol. 50, no. 4, pp. 130–138, 2022.

[3] G. H. Chen, P. Yang, Y. X. Zhao, X. F. Li, and Y. F. Zhang, "Vulnerability analysis of storage tank under the coupling effect of temperature load and blast fragment impact load," *Chemical Industry and Engineering Progress*, vol. 40, no. 2, pp. 1130–1136, 2021.

[4] G. H. Chen, Y. X. Zhao, L. X. Zhou, P. Yang, T. Zeng, and Y. F. Zhang, "Vulnerability analysis of storage tank considering protective layer under impact of blast fragment," *Chemical Industry and Engineering Progress*, vol. 39, no. 11, pp. 4750–4755, 2020.

[5] X. M. Ye, Z. M. Zhang, and L. Wan, "Analysis of seismic fragility parameter of fluid–filled container," *Atomic Energy Science and Technology*, vol. 53, no. 4, pp. 711–717, 2019.

[6] A. Aliche, H. Hammoum, K. Bouzelha, and N. E. Hannachi, "Development and validation of predictive model to describe the growth of concrete water tank vulnerability with time," *Periodica Polytechnica: Civil Engineering*, vol. 61, no. 2, pp. 244–255, 2017.

[7] L. J. Wei, X. Y. Wang, A. M. Luo, and Y. Xiang, "Investigation on seismic vulnerability of storage tanks based on Probit-bayes method," *Journal of Safety Science and Technology*, vol. 13, no. 11, pp. 17–21, 2017.

[8] S. Qi, *Research on Dynamic Response and the Vulnerability of Storage Tanks Influenced by Blast Fragments*, South China University of Technology, Guangzhou, China, 2017.

[9] J. G. Sun, R. H. Zhang, and F. Jiang, "Numerical simulation analysis on the seismic fragility of storage-tank," *Journal of Harbin Institute of Technology*, vol. 41, no. 12, pp. 138–142, 2009.

[10] Z. G. Li, *Numerical Modeling-Based Seismic Fragility Analysis of Base Isolation Vertical Storage Tanks*, Huazhong University of Science and Technology, Wuhan, China, 2013.

[11] H. Rong, S. Jin, and J. X. Gong, "Fragility analysis of nuclear power plant containment under near-site vibration," *Nuclear Power Engineering*, vol. 43, no. 2, pp. 126–132, 2022.

[12] D. Vamvatsikos and C. A. Cornell, "Incremental dynamic analysis," *Earthquake Engineering & Structural Dynamics*, vol. 31, no. 3, pp. 491–514, 2002.

[13] X. L. Lu, N. F. Su, and Y. Zhou, "IDA-based seismic fragility analysis of a complex high-rise structure," *Journal of Earthquake Engineering And Engineering Vibration*, vol. 32, no. 5, pp. 19–25, 2012.

[14] R. H. Zhang, *Seismic Fragility Study on the Vertical Storage Tanks Based on Reliability Theory*, Daqing Petroleum Institute, Daqing, China, 2009.

[15] M. S. Razzaghi and S. Eshghi, "Probabilistic seismic safety evaluation of precode cylindrical oil tanks," *Journal of Performance of Constructed Facilities*, vol. 29, no. 6, pp. 1–7, 2015.

[16] H. N. Phan, F. Paolacci, O. S. Bursi, and N. Tondini, "Seismic fragility analysis of elevated steel storage tanks supported by reinforced concrete columns," *Journal of Loss Prevention in the Process Industries*, vol. 47, pp. 57–65, 2017.

[17] B. Y. Zhang, Q. C. Li, W. Wang, and S. Z. Lu, "Dynamic response and failure mechanism of the large floating roof oil tanks under blast loading," *Journal of Harbin Institute of Technology*, vol. 46, no. 10, pp. 23–30, 2014.

[18] W. Jing, *Dynamic Responses and Seismic Response Reduction of Sliding Isolation concrete Rectangular Liquid Storage Structure*, Lanzhou University of Technology, Lanzhou, China, 2017.

[19] China Petroleum and Chemical Corporation, *Code for Seismic Design of Petrochemical Steel facilities(GB50761-2012)*, China Planning Press, Beijing, China, 2012.